Methodology and application to assess thermo-mechanical buckling in composite marine structures.

R. Pacheco[a,b,*], D. Di Capua[a,b], J. Garcia[a,b] and O. Casals[c]

[a] *International Center for Numerical Methods in Engineering (CIMNE), Gran Capitán s/n, 08034 Barcelona, Spain*
[b] *Polytechnic University of Catalonia (UPC), Barcelona, Spain*
[c] *Compass Ingeniería y Sistemas S.A., Spain*

ARTICLE INFO

Keywords:
Fire Safety, Thermo-Mechanical Analyses, Buckling, SPROM, Composite Materials and Marine Structures.

ABSTRACT

This paper describes the research performed within the scope of H2020 project FIBRE4YARD in the development of a suitable thermo-mechanical framework to analyse composite structures under fire loads. The thermo-mechanical model uses the adiabatic temperature to obtain the through-thickness distribution of temperature of the triangular shell element, this formulation is able to predict phenomena such as pyrolysis, thermo-mechanical yielding and large displacements (non-linear buckling). An application case of a load-bearing section of a container ship is shown to demonstrate the correctness of the methodology, two type of materials are considered in the analysis, traditional materials such steel and advanced materials like fibre reinforced plastic (FRP) composites.

1. INTRODUCTION

During the last decades, the International Maritime Organisation (IMO) and the European Union (EU) have clearly identified that one of strategical measures in the reduction of pollution, in particular green house gas (GHG) emissions, comes by the hand of modernising the current world fleet and the use of lightweight materials such as composites [1]. EU produces a 7.29% of the total GHG emissions of the world and similarly the international shipping accounts for a 2.13% [2], these percentages vary slightly with the one published by the IMO [3], nevertheless the common agreement is that a reduction in the shipping emissions will lead to a reduction in the global, and in particular, the EU emissions. This is specially true when considering that by 2030, the EU is expecting to achieve the 55% emission reduction compared to the pollution generated by the same time in 1990 [4].

The interest shown by the EU policies to reduce shipping transport emissions can be easily understood when observing Figure 1. Figure 1a shows that international shipping by 2020 takes almost 29% of the total EU emissions and compared to the emissions in 1990, almost a 20%. According to IMO, shipping emissions represent around a 13% of the overall EU GHG emissions [5]. Thus, a significant reduction in international shipping will be beneficial for the world and specially for the EU during the next ten years. This is the motivation behind different competitive projects such as [6], [7] or [8], which aim is to produce complete composite marine structures to demonstrate the significant advantages that this materials offer.

Modern shipping and one of the most common found in the EU is the transport of containers(see Figure 1b). The container ships represent almost a 25% of the total heavy fuel oil (HFO) consumed by international shipping. Therefore, in this work, a container ship will serve as a case of study to illustrate the significant changes in the design of such structures when considering composites.

*Corresponding Author : R. Pacheco
rafael.pacheco@cimne.upc.edu (R. Pacheco); dicapua@cimne.upc.edu (D. Di Capua); julio@cimne.upc.edu (J. Garcia); ovidi.casals@compassis.com (O. Casals)
www.cimne.com (R. Pacheco); www.compassis.com (O. Casals)
ORCID(s): 0000-0002-3837-2972 (R. Pacheco); 0000-0003-1201-8462 (D. Di Capua); 0000-0003-0160-7333 (J. Garcia)

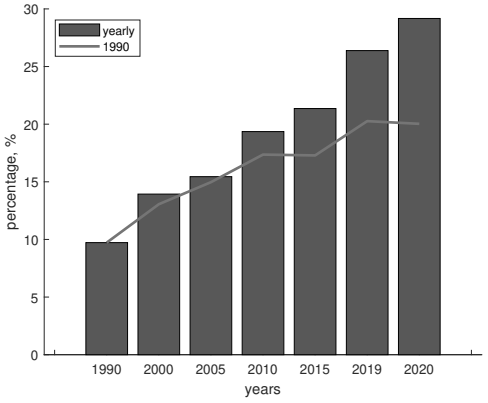

(a) The percentage that international shipping GHG emissions represents in terms of the European Union GHG [2].

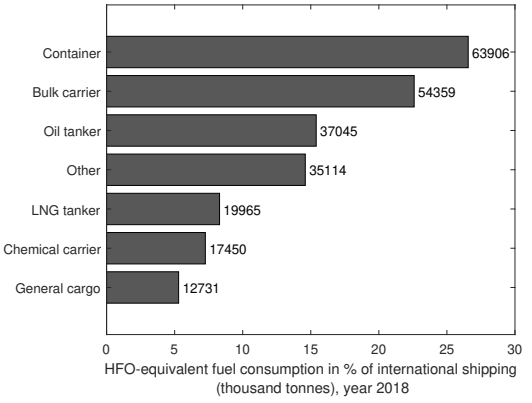

(b) Percentage and absolute magnitude that each vessel type represents from the total GHG emissions in international shipping [3].

Figure 1: Data of the green house gas emissions by the European Union and the international shipping.

Composite materials present advantages to traditional materials such as steel or aluminium (see Figure 2). The most common and known advantage is the amount of stiffness or robustness a structure can endure against its own density – the density by itself is a good indicator but not accurate enough – or e.i., the stiffness-weight ratio, which in the case of commercial composites is half of the steel and aluminium. In terms of mechanical response the yield strain, or the ratio between the yield strength and Young's modulus, is significantly higher in composites than steel or aluminium (about 30 times higher). This translates in the fact that composites can deform significantly more and still retain their elastic mechanical response, however, this is also a limitation in terms of computational modelling, since it involves a correct prediction of the *flexural nature of composites*, i.e., large displacements or non-linear geometric analysis. This is the reason why international association of classification societies (IACS) limit the slenderity of composite reinforcements and other structural members.

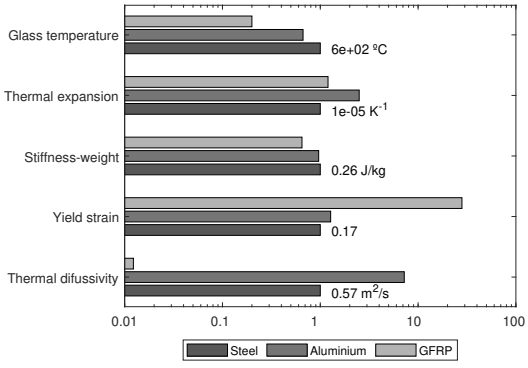

Figure 2: Thermal, mechanical and thermo-mechanical properties of steel, aluminium and glass fibre reinforced plastics. Each property is normalised with respect to the steel value. The horizontal axis is expressed in logarithmic scale.

When designing ships or other marine structures, one of the crucial aspects is the risk of fire, as explained in safety of life at sea (SOLAS). The construction of ships made out of composite is one of the most difficult subjects of study, since there is the incipient necessity of developing methodologies that correctly assess the behaviour of composites when exposed to fire. Specially focusing in the non-linear behaviour (constitutively and geometrically) of the thermo-

structural response. The key disadvantage of traditional composites is their ignition compared to steel or aluminium, specially for their lower glass temperature. Nevertheless, this risk is only high when considering a malfunction of the active fire protective systems and an incorrect design in the passive fire protective system (material configuration and scantlings). For instance, the risk of human life loss in structures of composites is very low when considering their outstanding thermal diffusivity, 1% the one of steel, which is a property that is intertwined with the amount of time it takes for a structure to reach a certain temperature, even considering that GFRP presents a glass temperature in the order 20% than steel, the amount of extra time before collapse in composite structures would be of roughly 5 times more than in steel. Another interesting property is that the thermal expansion of both composites and steel is very similar, so the thermo-mechanical response should be similar for the same range of temperatures, when no pyrolysis is involved.

Therefore, the purpose of this paper is to show the benefits in performance of composite structures against steel structures when fire is involved in the analysis. As mentioned previously, container ships are one of the most interesting vessels in terms of potential fuel reduction, considering the increase in the cargo transported when built using composites. Therefore, a hold of a container ship next to the engine room will be analysed, provided the fire will start in the engine room. This section under analysis will experiment significant fire and structural loads, which indeed will lead to high deflections and therefore the buckling phenomenology is also taken in consideration. The conclusions will revolve around the concept of *steel equivalent* found in SOLAS and how a correct passive fire protection design of the scantlings, configuration, stacking and insulation leads to a better thermo-structural response compared to traditional design.

2. Background research

In order to assess the integrity of composite structures, the use of a thermo-mechanical shell model will be employed [9]. This model uses a decoupled approach to first solve the non-linear one dimensional heat transient problem to obtain the distribution of temperature through the thickness and then solves the thermo-mechanical problem by taking into account the thermo-chemical degradation and induced damage in thermal and thermo-mechanical properties, respectively. It uses a micro-macro scale approach by taking into account the thermo-chemical processes at the constituent level, changes in fibre and matrix separately, and the prediction of the non-linear constitutive model of the composite is achieved by the so-called thermal serial-parallel rules of mixtures. A detailed scheme on how the solver works is described in Figure 3, it starts by solving the structural response pre-fire, then it divides the problem in different increments of times and for each, first the thermal problem is solved, by finding the temperature distribution through-thickness denoted by the variable 'x_3', and then the thermo-mechanical response.

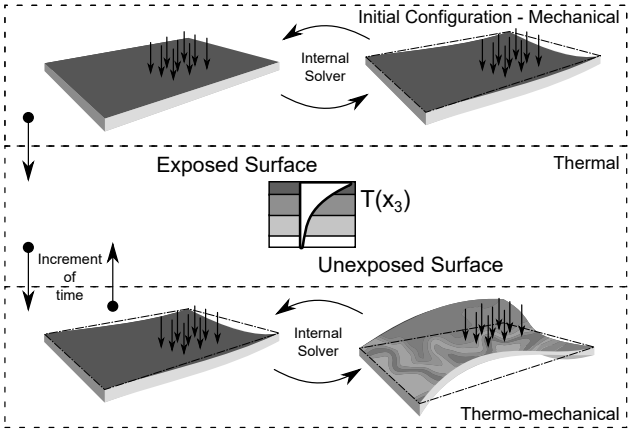

Figure 3: Scheme describing the thermo-mechanical coupling of the different modules of the thermo-mechanical solver.

The obtention of the boundary conditions will be based on the standard procedure of assuming a design fire curve. Figure 4 shows the stages of natural fire versus design fire curves (Figure 4a) and the difference between the hydrocarbon fire curve, that may be used in fires where the presence of this combustible is more probable, and the standard or ISO834 fire curve [10] (Figure 4b).

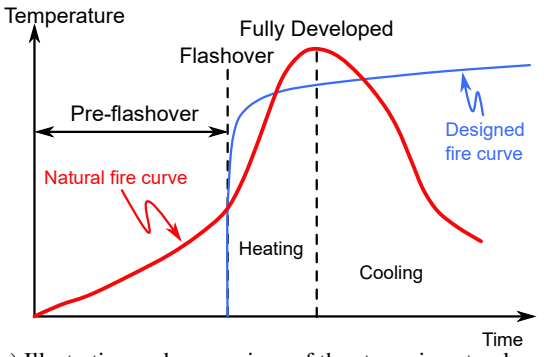

(a) Illustration and comparison of the stages in natural and design fire curves.

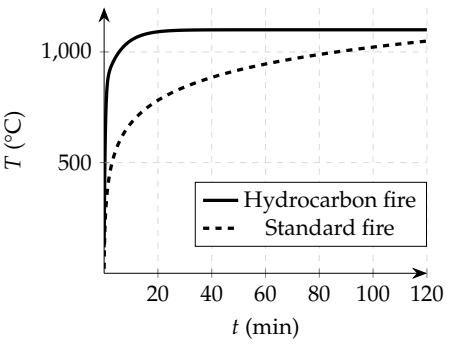

(b) Comparison between ISO834 and hydrocarbon curves, both are applicable to marine structure design.

Figure 4: Description of the boundary conditions by using the concept of design fire curves.

The difference between using a fire design curve and a direct numerical simulation , to obtain the fire dynamics, is in that the pre-flashover is underestimated, the peak temperature is reached slower, and the cooling phase is ignored. However, this means that in a significantly long fire scenario , the fire curves will be more restrictive than the natural solution. In the vast majority of regulations, the use of the ISO834 is enough to validate the passive fire protection system, nevertheless, if a more aggressive fire is preferred, in the presence of hydrocarbons as combustible, the hydrocarbon curve can be used instead.

These thermal boundary conditions are modelled using the concept of adiabatic surface temperature from [11], a non-linear one-dimensional heat transfer model introduced by Henderson et al. in [12]. The physics of the thermal problem are shown in Figure 5, the heat is considered to be transmitted in the boundary by convection and radiation and inside the thickness of the shell by conduction. Also, both, unexposed and exposed surfaces are considered to be radiant. Each layer of the composite stack can be compound of fibre and matrix, these two materials can be considered to pyrolise, starting from a virgin state of the properties to a charred or degraded state. The flow of the gas, generated from the matrix evaporation, is considered one-dimensional and prescribed from the unexposed surface to the exposed surface.

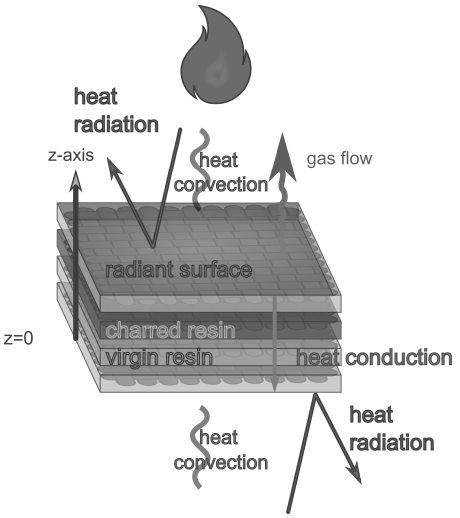

Figure 5: Illustration of the different elements involved in the non-linear one dimensional heat transfer problem.

When the temperature profile in the thickness of the shell is obtained, the thermo-mechanical analysis is updated and solved. The thermo-mechanical solver is based on the damage model originally from Simo and Ju [13], in particular the formulation found in [14, 15]. This method is the so-called isotropic damage model, a method that represents the non-linear rheology of a material based on a fluency criterion and a fracture energy constitutive law (see Figure 6).

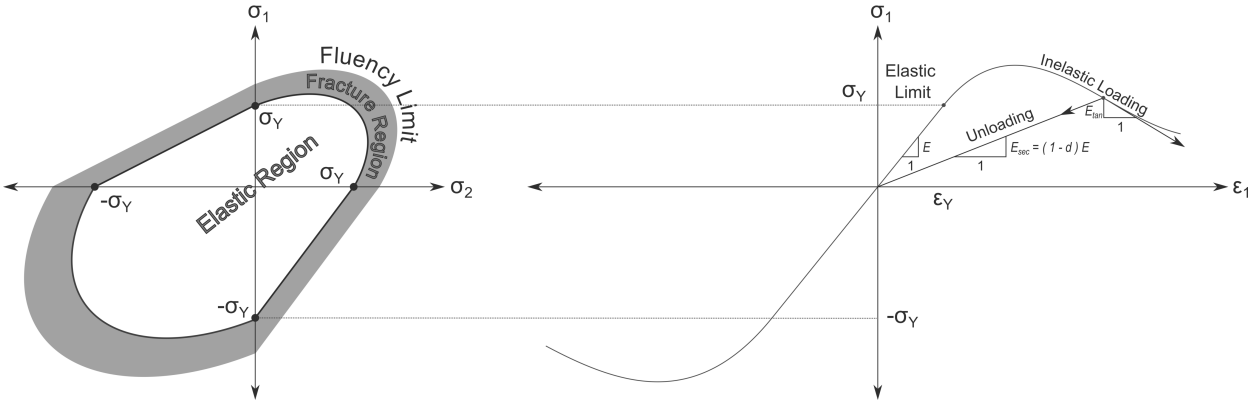

Figure 6: Representation of the isotropic damage model from [14]. Left: the fluency surface used in the evolution of the inelastic material behaviour.

The crack evolution at any discrete element is characterised by a damage parameter that ranges from zero or undamaged to one or completely damaged, this parameter is the ratio between the damaged or cracked section over the undamaged section as explained in Figure 7. The approach described in [9] applies the damage model to both matrix and fibre separately, this results in a higher degree of accuracy when predicting the mechanical response of a composite structure, since it is taking into account the inelastic behaviour at the microstructure level.

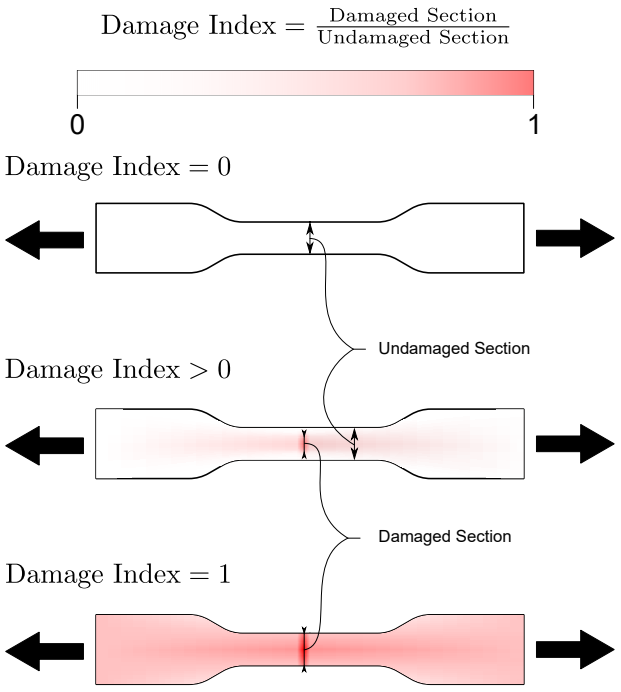

Figure 7: The concept of isotropic damage parameter for a simple tensile test. Observe the evolution of the damaged section in the centre of the specimen.

FRP composites are materials that present orthotropic constituent respones. In Figure 8, the in-plane stress and strain distribution presents two characteristic directions, the one aligned to the fibre or parallel direction, and transverse to the fibre orientation or serial direction. These characteristic directions were studied by Voigt and Reuss, who end up finding a way to define, explicitly, the constitutive modelling of composites based on the cosntitutive models of fibre and matrix materials. However, this explicit solution is not available when analysing the failure of composites.

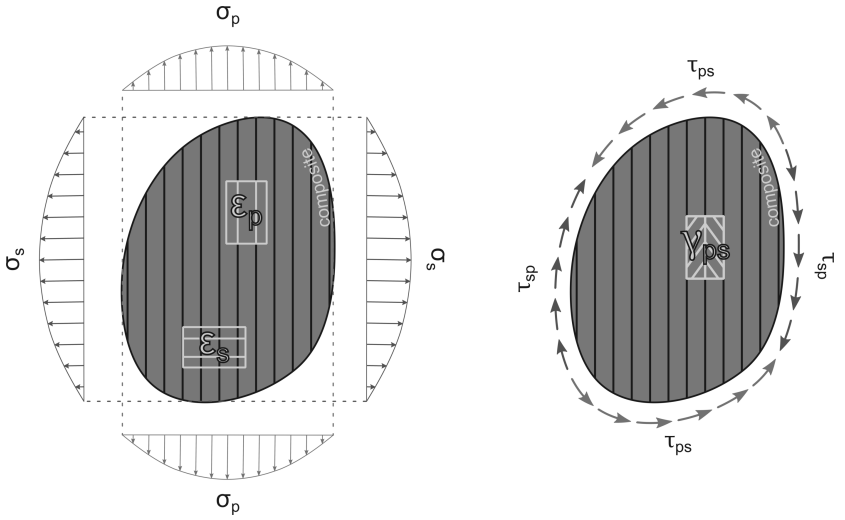

Figure 8: In plane stress distributions of an FRP composite. The stresses (σ) and strains (ε) are represented for both parallel and serial directions.

To be able to predict the failure of composites, the composite rheological model used in this paper is derived from the

application of the work of Rastellini et al. in [18], the so-called *serial-parallel rule of mixture* (SPROM). In special, the SPROM has been adapted to take into account the thermo-mechanical effects such as thermal expansion of fibre and matrix phases, thermo-chemical degradation of mechanical properties [19] and thermo-mechanical induced damage [20, 21] by temperature and also pyrolysis. This substantial modifications from the original SPROM theory are found in [9] and the final theory is renamed to *thermal serial-parallel rule of mixtures*.

3. Buckling

The formulation derived in [9] takes into account different non-linearities focused on constitutive modelling and degradation of both thermal and thermo-mechanical properties. However, the inherent flexibility of composites structures has to be taken into account to be able to check buckling. This is an important issue, since when structures are exposed to high temperature, their slender ratio, used to determine if a structure will yield or buckle, is significantly increased. This leads to thermal buckling and, in the case of considering non-linear constitutive phenomena such as damage, the analysis becomes inelastic thermal buckling.

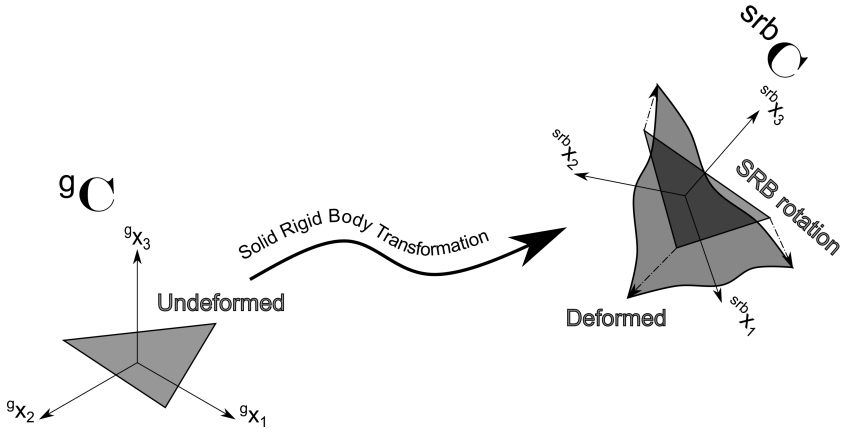

Figure 9: Interpretation of the different system of references used in the co-rotational theory.

The formulation used to address buckling, non-linear geometric buckling indeed, is best described in the research of Felippa and Haugen in [22]. The so-called co-rotational formulation, a formulation that introduces an intermediate system of references (see Figure 9) and the non-linear geometric dependency of the problem, is introduced in the transformation from the material system of reference to this intermediate system, also called solid rigid body system (SRB). The kinematics are then applied as per usual, but with respect to the SRB frame of reference. The mathematics are well documented in [22]. The general idea is that the description between the local and global displacements can be formulated as

$$^{G}\underline{a} = \underline{\underline{\Lambda}} \cdot {}^{L}\underline{a} \tag{1}$$

where a is the displacement vector and Λ is the transformation or rotation matrix. The notations ^{G} and ^{L} are the global and local frame of references, respectively. The non-linear geometric effect is then introduced in the rotation matrix, and this is decomposed in the product of three matrices that represent the solid rigid body movements of the intermediate axis.

$$\underline{\underline{\Lambda}} \left({}^{G}a\right)^{T} = \underline{\underline{\Lambda}}_{1}^{T} \cdot \underline{\underline{\Lambda}}_{2}^{T} \cdot \underline{\underline{\Lambda}}_{3}^{T} \tag{2}$$

where $\underline{\underline{\Lambda}}_{1}$, $\underline{\underline{\Lambda}}_{2}$ and $\underline{\underline{\Lambda}}_{3}$ are the three rotation matrices aforementioned. The description of these three can be found in

[23]. Then the system of equations for the thermo-structural problem is posed in its residual form as explained in [9] and the modification of the tangent stiffness due to non-linear geometric effects yields

$$\frac{\partial \underline{r}}{\partial a} = \frac{\partial \underline{\underline{\Lambda}}^T}{\partial a} {}^L\underline{F} + \frac{\partial {}^L\underline{F}}{\partial a} \underline{\underline{\Lambda}}^T \tag{3}$$

where F is the internal force vector. Note that the displacement and derivatives with respect to the displacement are considered with respect to the global coordinate system. Then the derivative of the internal force vector with respect to the displacement is equivalent to the material stiffness (K_M) and the derivatives with respect to the rotation matrices yield the non-linear geometric stiffness term.

$$\begin{cases} \dfrac{\partial {}^L\underline{F}}{\partial a} \underline{\underline{\Lambda}}^T \equiv {}^G\underline{\underline{K}}_M \cdot {}^G\underline{a} \\ \dfrac{\partial \underline{\underline{\Lambda}}^T}{\partial a} {}^L\underline{F} \equiv \left(\dfrac{\partial \underline{\underline{\Lambda}}_1^T}{\partial a} \cdot \underline{\underline{\Lambda}}_2^T \cdot \underline{\underline{\Lambda}}_3^T + \underline{\underline{\Lambda}}_1^T \cdot \dfrac{\partial \underline{\underline{\Lambda}}_2^T}{\partial a} \cdot \underline{\underline{\Lambda}}_3^T + \underline{\underline{\Lambda}}_1^T \cdot \underline{\underline{\Lambda}}_2^T \cdot \dfrac{\partial \underline{\underline{\Lambda}}_3^T}{\partial a} \right) \left({}^G\underline{\underline{K}}_M \cdot {}^G\underline{a} \right) = \\ \qquad \left({}^G\underline{\underline{K}}_{GR} + {}^G\underline{\underline{K}}_{GP} + {}^G\underline{\underline{K}}_{GM} \right) \cdot {}^G\underline{a} \end{cases} \tag{4}$$

where K_{GR}, K_{GP}, K_{GM} are the rotational geometric, equilibrium projection and moment-correction stiffnesses. The same notation can be found in [23]. Therefore, the non-linear geometric stiffness needed to simulate buckling can be then posed as

$${}^G\underline{\underline{K}}_{NG} = \left({}^G\underline{\underline{K}}_{GR} + {}^G\underline{\underline{K}}_{GP} + {}^G\underline{\underline{K}}_{GM} \right) \tag{5}$$

where K_{NG} is the non-linear geometric stiffness. The non-linear geometric buckling formulation is then completed and combined with the thermo-mechanical formulation for laminated shells exposed to fire described in [9].

4. Application to marine structures

To analyse buckling during a fire scenario, the approach used in [9] is employed. The model will take into account pyrolysis and damage, as well as thermo-mechanical degradation. To showcase the differences between steel and GFRP, two models are taken under consideration and two configurations of insulation are considered, with and without insulation. This aids to understand the difference between a negligible thermal insulation and correctly insulated one when it comes to the design of the passive fire protective system.

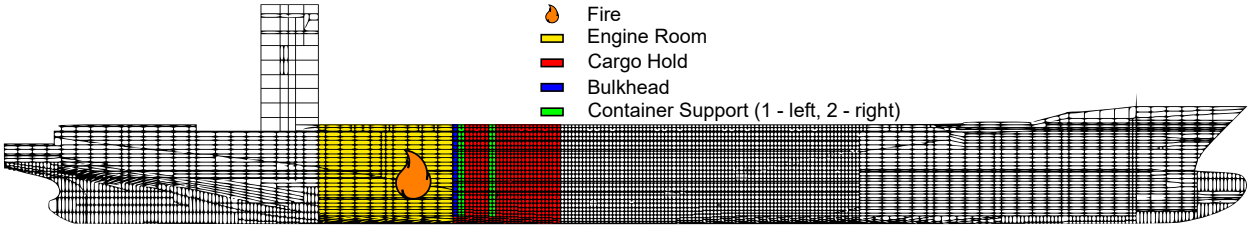

Figure 10: Description of the domain under study and the different arrangements found in it.

The analysis is performed on a container ship of the Panamax category, shown in Figure 10 and a close up of this section can be found in Figure 11. A fire will take place in the engine room and will rise the temperature of the adjacent

cargo hold by simple heat convection (Figure 11a). The hold presents three longitudinal load-bearing divisions and structures, a bulkhead that separates the engine room and the cargo hold, and two shelve-like structures, support 1 and support 2 (observe Figure 11b), where the rail mechanisms that hold the twenty-foot equivalent unit (TEU) containers are supported. These three rigid structures of interest are bearing a significant mechanical load that is unmodified by the temperature, thus, the capacity to assess buckling in these structures is of necessity as explained in the previous section.

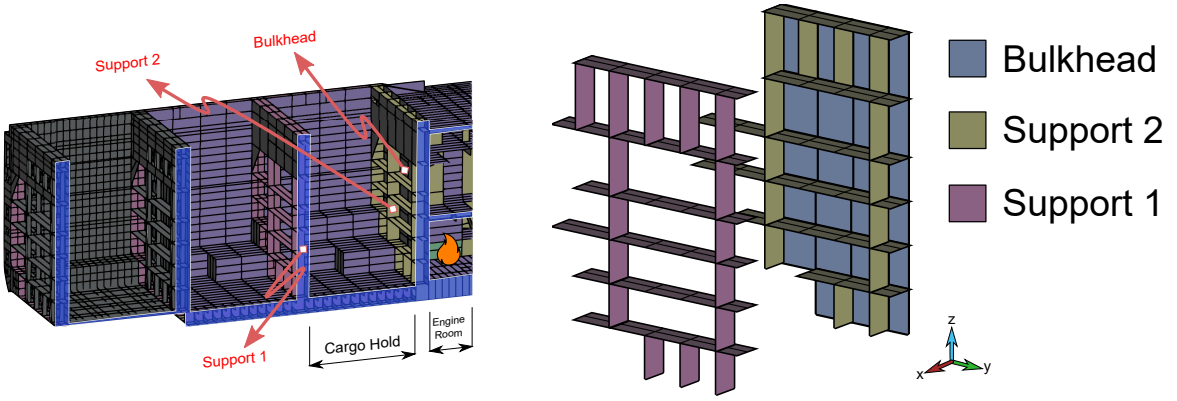

(a) Section under study. The blueish area represents a symmetric boundary condition.

(b) The three structures of interest that endure the major amount of the structural load in the cargo hold.

Figure 11: Computational domain under consideration in the analysis, left half of the real domain and right the region of interest inside this computational domain.

The integrity of the three structural members described in Figure 11b is assessed by the combination of two results obtained from the analysis. First, the thermo-mechanical damage index described in [9], an index that ranges from zero or intact integrity to one or collapsed integrity. This index is intrinsically interrelated to the secant stiffness of a given element, thus a value close to zero is analogous to an infinitely large displacement. However, since this analysis is subjected to considerable mechanical loads, the effect of buckling is also needed to be taken into account, since basing the analysis on pure yielding criteria might result in an incorrect passive fire protective design. Buckling is assessed by showing the deflection obtained in the structure and the index of damage. The methodology explained in this paper combines fire, yielding and large deflections, i.e., thermo-inelastic buckling.

The fire dynamics are modelled using a fire curve imposed in the engine room, close to the bulkhead. This fire curve is characterise by an ISO834 and a constant heat flux of 50 W/m^2, the fire is considered to transfer its heat by convection through the length of the ship and towards the cargo hold. The mechanism of fire is best illustrated in Figure 12, where the heat convection is assumed to be one dimensional and the temperature distribution at different points of the length are represented.

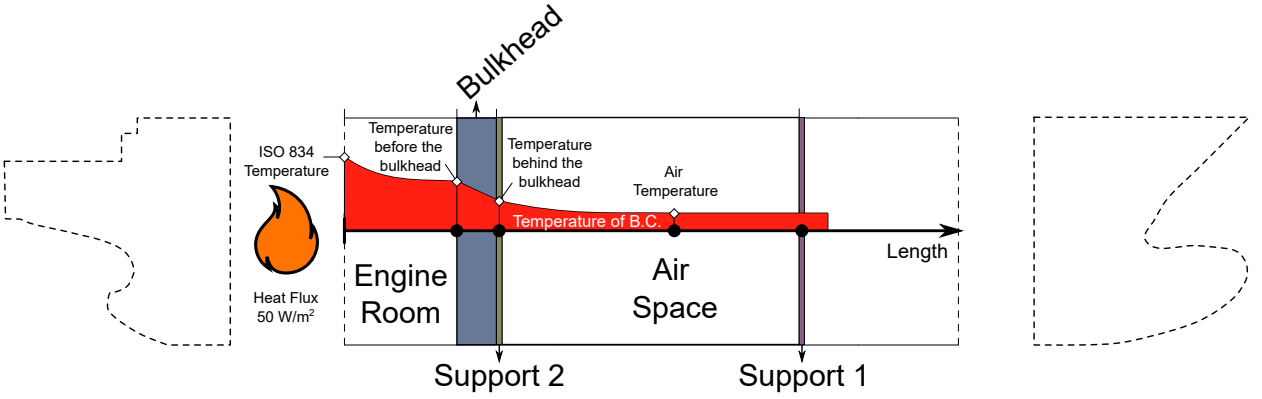

Figure 12: The spread of fire and how the temperature is distributed along the length of the ship.

Therefore, the thermal boundary conditions will be derived from considering that the dynamics of fire can be approximated by the solution of a one-dimensional heat transfer. In Figure 13 the flux and temperature is prescribed in the engine room. The only structural element of effective thermal resistance considered in the problem is the bulkhead, the conductivity resitance depends on the material under study. Also the convection resistance is considered, before the bulkhead (coefficient: $25W/m^2K$) and after the bulkhead (coefficient: $9W/m^2K$).

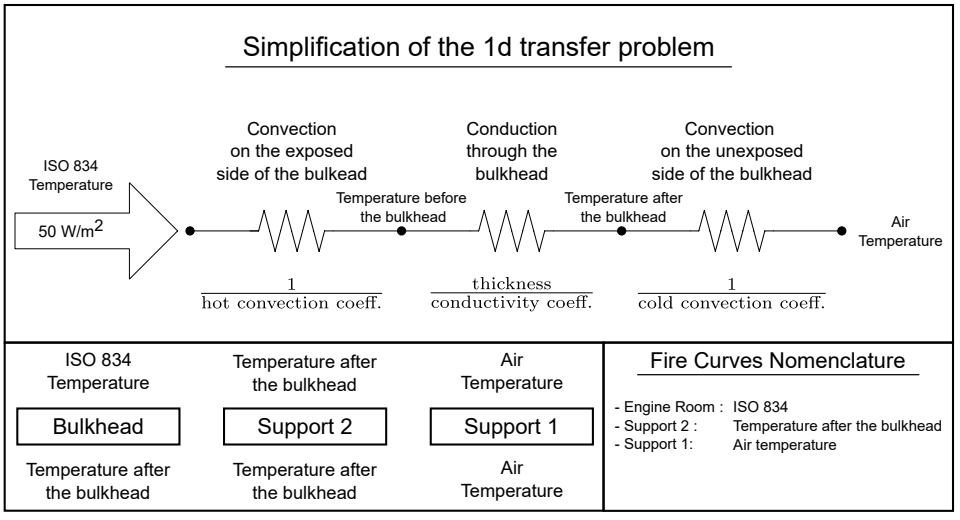

Figure 13: The mechanism of fire simplified. A description of the thermal resistances, temperature boundary conditions and nomenclature of the derived fire curves are shown.

The nomenclature described in Figure 13 describes the set of unique thermal boundary conditions used in the thermo-mechanical problem. The assumption is that the bulkhead will be exposed to a ISO 834 fire curve in its exposed side and to the temperature after the bulkhead in its unexposed side. The support 2, the one attached to the bulkhead, is exposed to the temperature after the bulkhead on all surroundings and the support 1, the furthest from the fire, is considered to be surrounded by the air of the compartment at a homogenised air temperature. When considering a correctly insulated configuration, the bulkhead presents insulation on both sides, therefore the temperature after the bulkhead and in the cargo hold is considered the ambient temperature ($20°C$).

From these assumptions, the thermal boundary conditions introduced in the thermo-mechanical analysis are three for each material configuration (see Figure 14), the ISO 834 that will be the engine room fire curve, the temperature after

the bulkhead that will be the support 2 fire curve, although it is also imposed behind the bulkhead as well. And the air temperature that will be renamed to support 1 fire curve.

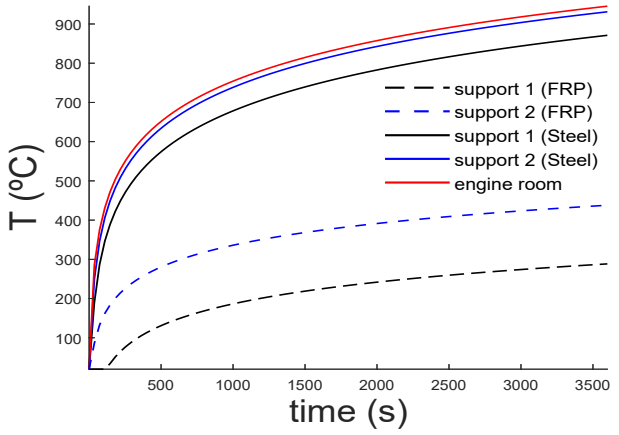

Figure 14: The thermal loads applied to the different compartments of the container ship.

It can be rapidly appreciated that for the same type of fire happening in the engine room, it is the FRP material the one that insulates better the cargo hold. From SOLAS, the concept of *steel equivalent* material focuses on obtaining at least the same performance, however, this shows that composites have ahigher performance, by delaying and giving more time to act on the development of fire.

Furthermore, from the mechanical aspect, the scantling of the composite is five times less if Figure 15 is taken into consideration. This is the result of considering that the *equivalent steel* criterion refers mechanically to the avoidance of yielding in any structural member, without yet taking into account buckling criteria. Generally, IACS regulation forbid the design of such thin structures since they are very prone to buckling. The properties of these two configurations are found in Table 1, Table 2 and Table 3. Note that the insulation is characterised by a rockwool type of material and is applied to both sides of the shell structures, it presents a significant low conductivity, reducing the heat transfer rate, it cannot pyrolise and its contribution to the thermo-mechanical response is little.

material	conductivity (W/m°K)	specific heat capacity (J/kg²°K)	gas specific heat capacity (J/m²°K)	density (kg/m³)	decomposition heat (W/kg)
glass fibre	0.5	800	0	2600	0
vinylester	0.2	1800	2200	1000	$4.5{\cdot}10^5$
steel	50	450	0	7800	0
rockwool	0.03	1000	0	60	0

Table 1
Thermal properties.

material	pre-exponential factor (s^{-1})	activation energy (J/mol)	order of reaction (J/m²°K)	char density (kg/m³)
GFRP	$6{\cdot}10^{20}$	$2.8{\cdot}10^5$	6	360

Table 2
Pyrolysis properties.

material	Young modulus		Poisson ratio	yield strength		fracture energy	glass temperature	curve fitting		thermal expansion
	virgin	charred		virgin	charred			1	2	
	(GPa)		-	(MPa)		(N/m)	($°C$)	-	-	($\cdot 10^{-6\circ} K^{-1}$)
glass fibre	72.4	0.7	0.21	1800	180	$1.2{\cdot}10^4$	100	0.06	6	12
vinylester	3.35	0.03	0.26	20	2	$8.0{\cdot}10^5$	100	0.06	6	12
steel	210	21	0.28	420	30	$5.0{\cdot}10^3$	600	0.01	6	10
rockwool	0.002	-	0	-	-	-	-	-	-	-

Table 3
Thermo-mechanical properties.

The computational mesh generated is described next. The thermo-mechanical analysis is implemented in the commercial software *TDYN Ramseries.* The time scheme is subdivided in steps of 100 seconds and one hour of study is considered, the simulation time is selected based on the desired structural subdivision class in terms of fire. SOLAS establishes different grades of fire protection depending on the thermo-mechanical response of the structural members, these classes are defined according several considerations, one of those is the elapsed time before collapse. The scope of this analysis was to determine if the configurations under consideration where able to endure at least 60-minutes fire scenario in the attempt to obtain an *A-60* class according to SOLAS.

The shells are discretised with 100 uniform divisions in thickness to capture well the thermal dynamics, and the overall spatial domain is discretised by 104513 elements and 97234 nodes, with an average triangular element size of 20 cm (see Figure 16). The average computational time for each simulation is between 4h and 6h, this depends on the material configuration, the composite model considers a micro-scale approach (simulation of fibre and matrix separately), on the amount of damage generated in the structure or in the thermal degradation processes happening inside the thickness of the structural members.

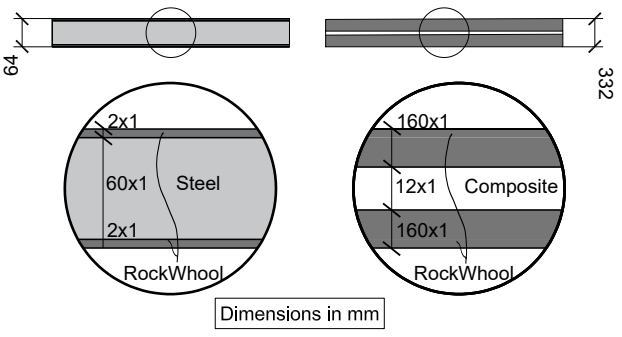

Figure 15: Configuration for the steel and FRP material stack in the bulkhead.

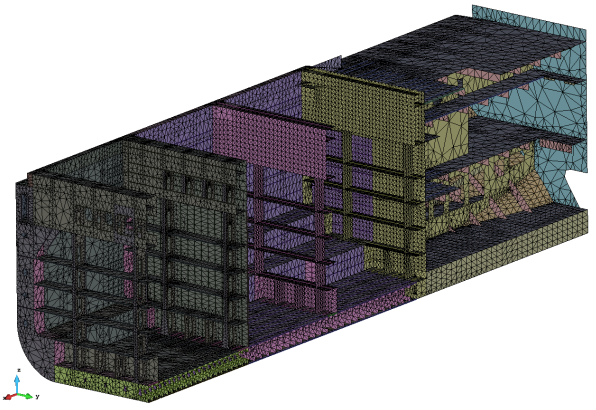

Figure 16: Mesh of the computational domain.

The results from the four cases under consideration are depicted in Figure 17. There are two dimensions of interest, the difference between the two materials, lightweight advanced materials and traditional materials, and the difference between what constitutes a bad insulation, and therefore a bad passive fire protection design, and an optimal insulation configuration. First note that since steel is non-flammable, the amount of insulation to withstand the fire load is significantly smaller given the one found in composites (Figure 15), that is used to avoid the ignition during one hour of exposition to the fire. The snapshots shown correspond to the analysis of the raw or non-insulated steel (620 seconds), insulated steel (3600 seconds), raw FRP (590 seconds) and insulated FRP (3600 seconds).

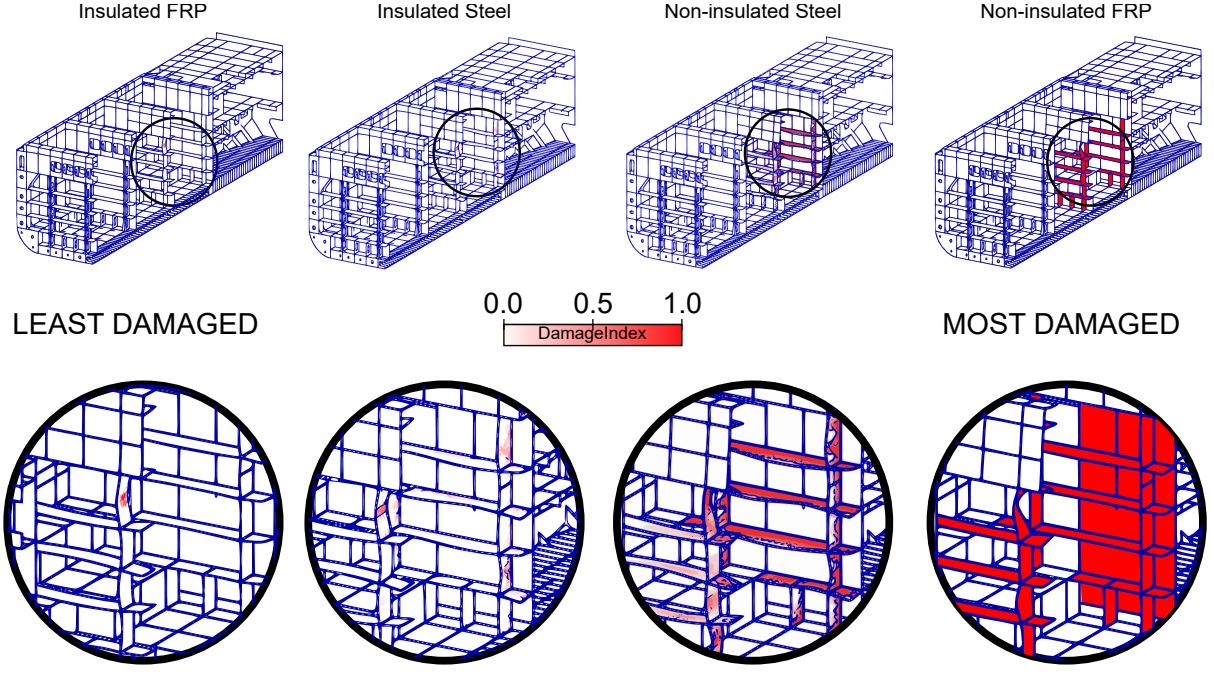

Figure 17: Computational results, combination of both mesh deformation and damage integrity. From the left (least damaged) to right (most damage) thermo-mechanical response.

Starting to evaluate the consequences of the fire scenario when both materials are non-insulated, it is clear that when the FRP configuration lacks of insulation, it is the worst possible kind of configuration. It only withstands until 590 seconds of the total 1h analysis, and then it loses all convergence, which is equivalent to complete collapse, i.e., as

the bulkhead and the two supports loss stiffness, and are the most rigid elements in the section, the other structural members present in the section are forced to endure the load since they become relatively stiffer compared to the degraded ones. This reaches to a point that the load is unable to be redistributed any longer and the structure collapses, i.e., the solver becomes unstable. It is fair to point out, that in normal circumstances, for passive design, the integrity criteria (damage index) should by no means surpass values over 20% or similar, what is shown here is the capability of the methodology to go beyond this scope and assess non-linear response. Indeed, the solution shows not only that the bulkhead and both supports have yielded, but also in support 1, buckling or post-buckling of a vertical member at the top of the shelf is observed.

In the case of steel without or poorly insulated, the distribution of damage is significantly high at 620 seconds, nevertheless, it is obvious that the integrity is better than the one of the non-insulated FRP. The steel case also collapses at that given time, which is slightly higher than composite, which is interesting, since composites present a glass temperature significantly lower than the ductile temperature of steel (around 600 $^{\circ}C$), this proofs that even badly insulated, the low thermal diffusivity of composites plays a key role on slowing the heat rate of the exposed structure. In the case of the non-insulated steel, there is some minor buckling or post-buckling in similar areas as in the FRP, however, the deflection is smaller.

If considering an adequate insulation of both configurations, steel shows three spots of damage that affect the integrity of the structure, the same spot that clearly buckled has buckled this time again, and two more spots in support 2 that present some damage pattern. The difference is that the structure has survived the fire scenario for at least one hour, and this would be close to obtain a higher fire grade classification (e.g., an *A-60* according to SOLAS).

In the case of the insulated FRP, the solution shows that composites, when correctly insulated, withstand much better fire, as there is no damage anywhere else than the top vertical member of the support 1. This support again has undergone buckling at some point and entered to post-buckling stage. However, the deflection is smaller than the one observed in the case of the insulated steel. Analogously, the structure has not collapsed and this would be eligible of a high fire grade classification, still improvable.

5. Conclusions

This paper has shown the capabilities of the framework and methodology described in order to assess the integrity of steel or laminated structures when exposed to fire and mechanical loading. The aspects of buckling were shown to be satisfactorily reproduced, thus proving the capabilities to not only address the yielding effects in composites, but to also take into the account of buckling and the combination of both, something that is remarkably unique in the current paradigm of research.

Since the current demand in research and production is the capability of producing large-length ships and marine structures that are lightweight, in order to minimise the environmental impact these have, the application has devoted to the comparison of the thermal and thermo-mechanical aspects that composites have with respect to traditional steel solutions. The low thermal diffusivity is an evident advantage, as well as their resistance to corrosion. When yielding criteria is examinated, composites present a significantly higher, almost 30 times, yield strain threshold compared to steel. This mechanical aspect is very interesting, albeit regulations forbid very thin laminate structures to be designed, the criteria is a result of the flexibility of composites, so the hidden criterion is fixed on buckling rather than yielding. This difference is clearly reflected on the thinner scantling used in this example, which in a practical case, would be higher to suffice the legal requirements. Nevertheless, the simulations have shown that with the right tools and theoretical models, thin composite structures are as safe as steel.

In conclusion, regardless the thickness used in the scantlings, composites can offer better thermo-structural performance when correctly insulated if compared to their *steel equivalent* solution. The concept of *steel equivalent*, although well defined, sometimes is very limited just to thermal aspects, without taking into consideration thermo-mechanical aspects as well.

6. Acknowledgement

This work was funded thanks to H2020 project FIBRE4YARD sponsored by the EUROPEAN COMMISSION under the grant agreement 101006860 "FIBRE composite manufacturing technologies FOR the automation and modular construction in shipYARDS". https://www.fibre4yards.eu/.

The scantlings of the container-ship model were provided by Daniel Sá and Manuel López.

		a	displacement [m]
${}^{G}A$	global notation	F	forceInt [N]
${}^{L}A$	local notation	r	residual [N]
$\underline{\underline{A}}$	matrix notation	Λ	rotationMatrix
$\underline{A}$	vector notation	K	stiffness [N/m]

References

[1] New materials to make ships more sustainable and less noisy for marine life | Research and Innovation, . URL https://ec.europa.eu/research-and-innovation/en/horizon-magazine/new-materials-make-ships-more-sustainable-and-less-noisy-marine-life.

[2] Crippa; M.; Oreggioni; G.; Guizzardi; D.; Muntean; Schaaf; E.; Lo Vullo; Solazzo; Monforti-Ferrario; F.; Olivier; J.G.J.; Vignati. GHG emissions of all world countries - 2021 Report, EUR 30831 EN. 2021. URL http://edgar.jrc.ec.europa.eu.

[3] Fourth IMO greenhouse gas study, .

[4] 2030 Climate Target Plan, . URL https://ec.europa.eu/clima/eu-action/european-green-deal/2030-climate-target-plan_en.

[5] Reducing emissions from the shipping sector, . URL https://ec.europa.eu/clima/eu-action/transport-emissions/reducing-emissions-shipping-sector_en.

[6] HOME - FibreShip. URL http://www.fibreship.eu/.

[7] FIBRE composite manufacturing technologies FOR the automation and modular construction in shipYARDS | FIBRE4YARDS Project | H2020 | CORDIS | European Commission. URL https://cordis.europa.eu/project/id/101006860/es.

[8] Development, engineering, production and life-cycle management of improved FIBRE-based material solutions for structure and functional components of large offshore wind enerGY and tidal power platform | FIBREGY Project | H2020 | CORDIS | European Commission. URL https://cordis.europa.eu/project/id/952966.

[9] R. Pacheco-Blazquez, D. Di Capua, J. García-Espinosa, O. Casals, and T. Hakkarainen. Thermo-mechanical analysis of laminated composites shells exposed to fire. *Engineering Structures*, 253, 2022. ISSN 18737323. doi: 10.1016/j.engstruct.2021.113679.

[10] ISO834:1. ISO - ISO 834-11:2014 - Fire resistance tests — Elements of building construction — Part 11: Specific requirements for the assessment of fire protection to structural steel elements, 3 2014. URL https://www.iso.org/standard/57595.html.

[11] Wickstrom Ulf, Dat Duthinh, and Kevin Mcgrattan. Adiabatic Surface Temperature for Calculating Heat Transfer To Fire Introduction. *Most*, 2, 9 2007. URL https://www.nist.gov/publications/adiabatic-surface-temperature-calculating-heat-transfer-fire-exposed-structures.

[12] J.B. Henderson, J.A. Wiebelt, and M.R. Tant. A Model for the Thermal Response of Polymer Composite Materials with Experimental Verification. *Journal of Composite Materials*, 19(6):579–595, 11 1985. ISSN 0021-9983. doi: 10.1177/002199838501900608. URL http://journals.sagepub.com/doi/10.1177/002199838501900608.

[13] J. C. Simo and J. W. Ju. Strain- and stress-based continuum damage models-I. Formulation. *International Journal of Solids and Structures*, 23 (7):821–840, 1987. ISSN 00207683. doi: 10.1016/0020-7683(87)90083-7. URL http://www.sciencedirect.com/science/article/pii/0020768387900837.

[14] R. Faria, J. Oliver, and M. Cervera. A strain-based plastic viscous-damage model for massive concrete structures. *International Journal of Solids and Structures*, 35(14):1533–1558, 1998. ISSN 00207683. doi: 10.1016/S0020-7683(97)00119-4. URL http://www.sciencedirect.com/science/article/pii/S0020768397001194.

[15] J. Oliver. A consistent characteristic length for smeared cracking models. *International Journal for Numerical Methods in Engineering*, 28 (2):461–474, 2 1989. ISSN 10970207. doi: 10.1002/nme.1620280214. URL http://doi.wiley.com/10.1002/nme.1620280214.

[16] W. Voigt. Ueber die Beziehung zwischen den beiden Elasticitätsconstanten isotroper Körper. *Annalen der Physik*, 274(12):573–587, 1889. ISSN 15213889. doi: 10.1002/andp.18892741206. URL http://onlinelibrary.wiley.com/doi/10.1002/andp.18892741206/abstract.

[17] A. Reuss. Berechnung der Fließgrenze von Mischkristallen auf Grund der Plastizitätsbedingung für Einkristalle . *ZAMM - Journal of Applied Mathematics and Mechanics / Zeitschrift für Angewandte Mathematik und Mechanik*, 9(1):49–58, 1929. ISSN 15214001. doi: 10.1002/zamm.19290090104. URL http://doi.wiley.com/10.1002/zamm.19290090104.

[18] Fernando Rastellini, Sergio Oller, Omar Salomón, and Eugenio Oñate. Composite materials non-linear modelling for long fibre-reinforced

laminates. *Computers & Structures*, 86(9):879–896, 5 2008. ISSN 00457949. doi: 10.1016/j.compstruc.2007.04.009. URL https://linkinghub.elsevier.com/retrieve/pii/S0045794907001642.

[19] A P Mouritz and A G Gibson. *Fire Properties of Polymer Composite Materials*, volume 143 of *Solid Mechanics and Its Applications*. Springer Netherlands, Dordrecht, 2006. ISBN 978-1-4020-5355-9. doi: 10.1007/978-1-4020-5356-6. URL http://link.springer.com/10.1007/978-1-4020-5356-6.

[20] Miguel Cervera, Javier Oliver, and Tomás Prato. Thermo-Chemo-Mechanical Model for Concrete. II: Damage and Creep. *Journal of Engineering Mechanics*, 125(9):1028–1039, 9 2002. ISSN 0733-9399. doi: 10.1061/(asce)0733-9399(1999)125:9(1028). URL http://ascelibrary.org/doi/10.1061/%28ASCE%290733-9399%281999%29125%3A9%281028%29.

[21] Miguel Cervera Ruiz, Xavier Oliver Olivella, and T Prato. Thermo-chemo-mechanical model for concrete. II: damage and creep. *Journal of engineering mechanics*, 125(9):1028–1039, 9 1999. ISSN 0733-9399. doi: 10.1061/(ASCE)0733-9399(1999)125:9(1028). URL https://upcommons.upc.edu/handle/2117/192645.

[22] Carlos A. Felippa and Bjorn Haugen. A unified formulation of small-strain corotational finite elements: I. Theory. *Computer Methods in Applied Mechanics and Engineering*, 194(21-24 SPEC. ISS.):2285–2335, 6 2005. ISSN 00457825. doi: 10.1016/j.cma.2004.07.035.

[23] F S Almeida and A M Awruch. Corotational nonlinear dynamic analysis of laminated composite shells. 2011. doi: 10.1016/j.finel.2011.05.001. URL www.elsevier.com/locate/finel.